Composition and emission factors of traffic- emitted intermediate volatility and semi-volatile hydrocarbons (C_{10}–C_{36}) at a street canyon and urban background sites in central London, UK

Xu, Ruixin; Alam, Mohammed S.; Stark, Christopher; Harrison, Roy M.

DOI:
10.1016/j.atmosenv.2020.117448

Document Version
Peer reviewed version

Citation for published version (Harvard):
Xu, R, Alam, MS, Stark, C & Harrison, RM 2020, 'Composition and emission factors of traffic- emitted intermediate volatility and semi-volatile hydrocarbons (C_{10}–C_{36}) at a street canyon and urban background sites in central London, UK', *Atmospheric Environment*, vol. 231, 117448.
https://doi.org/10.1016/j.atmosenv.2020.117448

Composition and Emission Factors of Traffic-Emitted Intermediate Volatility and Semi-Volatile Hydrocarbons (C_{10}-C_{36}) at a Street Canyon and Urban Background Sites in Central London, UK

Ruixin Xu, Mohammed S. Alam, Christopher Stark and Roy M. Harrison*†

Division of Environmental Health and Risk Management, School of Geography, Earth and Environmental Sciences University of Birmingham Edgbaston, Birmingham B15 2TT United Kingdom

* To whom correspondence should be addressed.
Tele: +44 121 414 3494; Fax: +44 121 414 3709; Email: r.m.harrison@bham.ac.uk

†Also at: Department of Environmental Sciences / Center of Excellence in Environmental Studies, King Abdulaziz University, PO Box 80203, Jeddah, 21589, Saudi Arabia

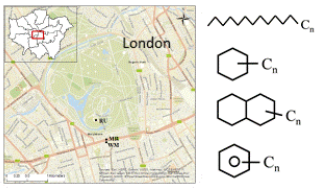

TOC CAPTION: The measurements of I/SVOCs in the London Campaign 2017.

ABSTRACT

Hydrocarbons in both gas and particle phases from C_{10} to C_{36} (I/SVOCs) were analysed at sites in central London. Samples were collected from a street canyon, Marylebone Road (MR), a rooftop site (WM) above MR, and a site in the adjacent Regent's Park (RU), north of MR to evaluate the change in composition of I/SVOCs during advection from the traffic to the cleaner atmosphere of the urban background. Groups of compounds identified and quantified in gas and particle phases include C_{13}-C_{36} n-alkanes and branched alkanes, C_{12}-C_{25} monocyclic alkanes, C_{13}-C_{27} bicyclic alkanes and C_{10}-C_{24} monocyclic aromatics. The similarities found in the aliphatic and aromatic region above C_{12} in urban air and diesel exhaust demonstrate the impact of diesel-powered vehicles on urban air quality. Diesel exhaust is suggested to be the dominant emission source, while small differences between sites indicate the possibility of other sources which are also discussed. The ambient concentrations of I/SVOCs in the street canyon at MR were highest when the southerly winds brought the traffic emitted pollutants to the sampler. Emission factors (EFs) for all compound groups were estimated from the concentrations at the MR site. Particle-phase n-alkane EFs are broadly similar to those measured elsewhere in the world, despite differences in traffic fleet composition. A comparison between n-alkane EFs estimated from field measurements and those measured from diesel engines in the laboratory suggests a large contribution from vehicles with higher emissions than recent passenger cars to London air.

Key Words: Hydrocarbon; semi-volatile; diesel emission; street canyon; emission factor

1. INTRODUCTION

Particulate matter is the air pollutant with the greatest public health impact, and its effects are likely to depend upon particle size and composition (Rissler et al., 2012; Masiol et al., 2012). As a major emission source within the urban environment, particulate matter originated from traffic has generated major interest over the last few decades. The majority of traffic-emitted fine particles are carbonaceous, directly emitted as primary organic aerosol (POA) and elemental carbon, oxidation of the former leading to production of secondary organic aerosol (SOA) (Jimenez et al., 2009). A substantial fraction of the organic compounds in exhaust emissions of gasoline and diesel vehicles are semi-volatile (May et al., 2013a,b). While intermediate volatility organic compounds (IVOCs) exist mainly in the vapour phase, semi-volatile organic compounds (SVOCs) partition directly between gas and particulate phases under ambient conditions (May et al., 2013a; Robinson et al., 2007; Donahue et al., 2012). SVOCs refer to organic species with an effective saturation concentration C^* between 1 and 10^3 μg m^{-3} while IVOCs refer to species with C^* between 10^4 and 10^7 μg m^{-3} (Robinson et al., 2007).

I/SVOC emissions from traffic mainly comprise aliphatic and aromatic hydrocarbons typically ranging between C_{12} and C_{35} (Worton et al., 2014; Gentner et al., 2012; Alam et al., 2018; Weitkamp et al., 2007). Most of the gasoline emitted organic compounds are volatile organic compounds (VOCs) while some aromatics can extend to the intermediate-volatile range. Only 30% of diesel emitted hydrocarbons are VOCs and most of them are less volatile (mainly I/SVOCs) (Gentner et al., 2012). Gasoline engine emissions are typically in the carbon number range below C_{12} while diesel engine emissions are mainly in the range from C_8 to C_{25} (Gentner et al., 2012). Detailed emission information for these diesel-derived organic compounds (above C_{12}) in the atmosphere is not widely available (Dunmore et al., 2015) although the greatest roadway emitters of particles per vehicle are diesel powered. In the UK, 40% of licensed passenger cars were using a diesel engine in 2017 (Fleet News, 2018). Diesel exhaust contains primarily unburned fuel (C_{15}-C_{23}

74 organics), unburned lubricating oil (C_{15}-C_{36} organics) and sulfate (Jacobson et al., 2005). A recent
75 study investigated the hydrocarbon composition of diesel exhaust using gas chromatography
76 coupled with time-of-flight mass spectrometry and concluded that the diesel fuel contributes up to
77 C_{20} hydrocarbons whilst engine lubricating oil contributes primarily to the C_{18} to C_{36} range of
78 compounds (Alam et al., 2016a).

79

80 Despite huge research interest and many contributions over the last decades, many uncertainties
81 remain regarding the identities and chemical composition of traffic emitted I/SVOCs. A key reason
82 is that the vast majority of I/SVOC mass cannot be separated and characterised by the traditional
83 one-dimensional gas-chromatography (1D-GC) based analytical techniques (Schauer et al., 1999;
84 2002; Jathar et al., 2012). A mixture of cyclic, linear, and branched hydrocarbons is present in a
85 typical chromatogram as an unresolved complex mixture (UCM) (Mandalakis et al., 2002). The
86 UCM is often observed in samples associated with the use of fossil fuels (Nelson et al., 2006;
87 Frysinger et al., 2003; Ventura et al., 2008), and comprises more than 80% of the semi-volatile
88 hydrocarbons emitted from diesel and gasoline derived engines (Schauer et al., 2002; 1999; Chan et
89 al., 2013). A number of studies have reported the chemical components of organic emissions in
90 traffic influenced regions by using one dimensional chromatography coupled with mass
91 spectrometry (GC-MS) or comprehensive two-dimensional gas chromatography coupled with mass
92 spectrometry (GC×GC -MS) (Lewis et al., 2000; Hamilton and Lewis, 2003; Omar et al., 2007;
93 Chan et al., 2013; Hamilton et al., 2004; Worton et al., 2014; Dunmore et al., 2015). However, the
94 homologous series that have been reported in most of the studies only represent a small fraction of
95 the total organic mass that is emitted from traffic, with a consequent lack of information on I/SVOC
96 composition.

97

98 Emissions from road traffic are known to make a large contribution to total particulate matter (van
99 Deursen et al., 2000) and vapour concentrations in urban areas. It is important to understand the

magnitude and characteristics of I/SVOC emissions from vehicles, especially in megacities like London. Measurements on laboratory-based diesel engines (Schauer et al., 1999; Perrone et al., 2014) allow the determination of exhaust emissions under controlled test conditions but these tests often cover a limited set of vehicles due to the high costs. These tests cannot fully represent the large variation in engine types and driving modes in different environments (Charron et al., 2019), and are not able to give an accurate estimation on the dilution of I/SVOCs (Kim et al., 2016) and do not include non-exhaust emissions (Pant et al., 2013). Therefore, estimates deriving from concentration measurements at a near-road site are considered to offer a realistic simulation for the emission factors, which currently comprise both tunnel and roadside measurements (Hwa et al., 2002; Kawashima et al., 2006; He et al., 2008, Staehelin et al., 1998).

In this study, samples were collected in central London at the roadside of the heavily trafficked Marylebone Road (MR), and two rooftop sites (WM and RU) during different times from January to April 2017 in London. The samples were analysed by using comprehensive two-dimensional gas chromatography time-of-flight mass spectrometry (TD-GC×GC-ToF-MS) combined with a mapping and grouping methodology to classify, identify and quantify the compounds classes. I/SVOCs (C_{10}-C_{36}) were identified and quantified in both the gas phase and particle phase, to offer a more comprehensive understanding of the chemical composition of traffic emitted particulate matter. The concentrations of four main I/SVOC groups are reported and discussed, including alkanes (n+i) (defined as the sum of n-alkanes and branched alkanes), monocyclic alkanes, bicyclic alkanes and monocyclic aromatics. The effect of wind direction on the dispersion of traffic emitted pollutants in the street canyon and the spatial distribution of I/SVOCs in different locations are discussed. Emission factors for n-alkanes and the main I/SVOC groups are estimated for traffic on Marylebone Road. Oxygenates, which are both important primary emissions from road traffic, and are formed by atmospheric oxidation of hydrocarbons have been addressed in an earlier paper (Lyu et al., 2019).

2. EXPERIMENTAL

2.1 Field Measurements in London Campaign, 2017

Simultaneous measurements were conducted on the roof of the University of Westminster (WM) and a roof of Regent's University (RU) from 24 January 2017 to 19 February 2017. The WM sampling site was located on the roof of a Westminster University building (around 26 metres high) on the south side of the road overlooking the ground-level Marylebone Road (MR) monitoring station. The RU sampling site was located on the roof (around 16 metres high) of Regent's University located in Regent's Park, which is about 380 m north of Marylebone Road (see Figures S1 and S2). Samples were also collected at the kerbside MR Supersite on the south side of Marylebone Road from 22 March to 18th April 2017. Marylebone Road has three traffic lanes for each direction and the traffic flow is over 80,000 vehicles per day. The instruments were housed in a large cabin placed on the sidewalk of Marylebone Road with an inlet around 2.5 metres above ground level.

2.2 Sample Collection

An in-house auto-sampler was designed to collect sequential 24 h duration samples (Figure S3). The sampler has seven channels and is turned to the next channel automatically. A pump draws air through a polypropylene backed PTFE filter (47 mm, 1 µm pore, Whatman, Maidstone, UK) to collect the particulate phase, and then through a stainless steel thermal adsorption tube packed with 1 cm quartz wool and 300 mg Carbograph 2TD 40/60 (Markes International) to collect the gas phase. The flowrate was calibrated by a calibrator (Gilian Gilibrator-2 NIOSH Primary Standard Air Flow Calibrator, Sensidyne, Schauenburg, Germany) and set at 1.5 L/min during the field measurements. The inlet to the sampler was through a downward facing ¼ inch o.d. stainless steel tube giving an estimate cut point of around 4 µm (Harrison and Perry, 1986). After 24h duration sampling, filters were transferred to pre-cleaned filter cases which are then enclosed with aluminium foil. Adsorption tubes were capped firmly. Both filter cases and tubes were stored under

conditions of approximately -18℃ prior to extraction and GC×GC-ToF-MS analysis. Adsorption tube breakthrough was evaluated in the field with two tubes in series, and vapour concentrations are reported only for compounds for which collection was quantitative.

2.3 GC×GC ToF MS Analysis

A two-dimensional approach separating compounds in a mixture by volatility and polarity was adopted. The analytical instruments and calibration methods have been described in earlier papers from our group (Alam et al., 2016a,b; Alam and Harrison 2016, Alam et al., 2018). Nine deuterated internal standards namely, dodecane-d26, pentadecane-d32, eicosane-d42, pentacosane-d52, triacontane-d62, biphenyl-d10, n-butylbenzene-d14, n-nonylbenzene-2, 3, 4, 5, 6-d5 (Chiron AS, Norway) and p-terphenyl-d14 (Sigma Aldrich, UK) were used in this study.

Adsorption tubes were spiked with 1 ng of deuterated internal standard for quantification. Then the tubes were desorbed onto a cold trap at 350ºC for 15 min (trap held at 20ºC), and then the trap released chemicals into the column with a split ratio of 100:1 (split ratio changed based on sampling sites) at 350ºC. Carrier gas was helium at a constant flow rate of 1 ml/min. Whole PTFE filters were spiked with 5 µl internal standards (1 ng/µL) for quantification, and were extracted with dichloromethane (HPLC grade), using ultrasonic agitation at room temperature (20ºC) for 20 mins. The filtrate was concentrated using a stream of dry nitrogen gas, to a volume of approximately 50 µl. 1 µL of the extracted sample was injected with a split ratio of 100:1 (split ratio changed based on sampling sites) at 300ºC. A modulation time of 11s was applied while a total run time for each sample was 120 min. Subsequent data processing was conducted using GC Image_v2.6 (Zoex Corporation). Blank filters were prepared, processed, and analysed in the same manner as the real particle phase samples to mitigate the analytical bias and precision. More details of the instrument settings and sample analysis methods are given by Alam et al. (2016a,b).

2.4 Classification of Organic Compounds

Recently studies have reported that the diesel fuel derived organic compounds are predominantly found from C_{13}-C_{20}, while compounds derived from lubricating oil are predominantly within the range C_{18}-C_{35}. Both are part of an unresolved complex mixture (UCM) in traditional GC (Dunmore et al., 2015; Alam et al., 2016a,b). The number of possible structural isomers increases with the number of carbon atoms (Goldstein and Galbally, 2007), and beyond around C_9 it is a challenge to identify the structure of all compounds present in the ambient air (Dunmore et al., 2015). However, it is possible to assign individual compounds to particular chemical classes and functionalities based on their retention behaviour in two-dimensional chromatography. The physicochemical similarities within compound classes and their steady changes with the increasing chain length and /or molecular sizes enables the further identification of the ordered appearance of compounds in the chromatogram. This allows the identification of species without unique mass spectra but based on the pattern of the database. This study grouped the chemical compounds into isomer sets based on their carbon number and functional group (Figure 1). Natural standards were chosen for calibration and quantification, including n-alkanes (C_{11}-C_{36}), phytane and pristane (Sigma Aldrich, UK), n-alkyl-cyclohexanes (C_{11} -C_{25}), n-alkylbenzenes (C_{10}, C_{12}, C_{14}, C_{16} and C_{18}), tetralin, alkyl-tetralins (methyl-, di-, tri- and tetra-), cis- and trans-decalin, alkyl-naphthalenes (C_{11}, C_{12}, C_{13} and C_{16}) (Chiron AS, Norway) and 13 polycyclic aromatic hydrocarbons (Thames Restek UK Ltd). The authentic standard mixture (72 natural standards and 9 internal standards) was expected to cover as much of the whole chromatogram as possible and can be applied to calibrate the quantification of the isomer groups with the same functionality and molecular ions. Briefly, known amounts of natural and internal standard were injected into the GC×GC -MS system prior to the sample analysis to determine the response of target compounds. The identification of individual compounds is described by Alam et al. (2016b). Groups of isomers were quantified by adopting an individual compound with the same carbon number and functionality as a surrogate. For instance, the response for n-tridecane, (*m/z* 184) was used to quantify all isomers identified within the C_{13} alkane polygon.

More mapping details are given in Supplementary Information, Section 2.The quantification of isomer sets has been discussed in Alam et al., (2018), who reported the overall uncertainties of this method as 24% by comparing the difference between concentrations estimated with authentic standards and generic standards.

2.5 Supporting Data

The DEFRA air quality network (https://uk-air.defra.gov.uk/networks/) measures black carbon (BC), NO_x and benzene concentrations at the Marylebone Road monitoring station (MR) used in this study. Measurements of BC at the roof sites WM and RU were carried out using aethalometers (2 Wavelength Magee Aethalometer AE22) simultaneously with I/SVOC measurements.

London Heathrow airport, located west of central London, is the closest station to provide comprehensive meteorological information for the sampling sites above the roof. Daily mean wind direction data from London Heathrow airport (Met Office, 2006) were used to sort the 24 h duration I/SVOC samples into north wind (N), south wind (S) and undefined wind (Duffy and Nelson, 1996) based on the predominant direction during each sampling interval. The wind angles 300-360° and 0-60° are defined as a north wind while wind angles 120-240º are defined as a south wind in this study. North wind and south wind are both cross-canyon flows, whilst an undefined wind (Duffy and Nelson, 1996) represents the along-street flows, including wind angles $60-120°$ (east wind) and 240-300° (west wind). The Heathrow site is within 25 km of the London sampling sites. Using data from UK sites, Manning et al. (2000) show that wind data from airfield sites are representative of wind fields up to 40 km from the site. The Heathrow data represent winds above the street canyon; those within the canyon are very different. Harrison et al. (2019) show diagrammatically the circulations within the Marylebone Road canyon.

3. RESULTS AND DISCUSSION

3.1 I/SVOC Measured at MR and RU

3.1.1 Chemical composition and distribution

The identified and quantified chemical groups were C_{13}-C_{36} alkanes (n+i), C_{12}-C_{25} monocyclic alkanes, C_{13}-C_{27} bicyclic alkanes, C_{10}-C_{24} monocyclic aromatics, C_{10}-C_{15} naphthalenes, C_{13}-C_{15} biphenyls, C_{14}-C_{15} fluorenes, C_{15}-C_{16} phenanthrenes/anthracenes and C_{12}-C_{13} tetralins. Lyu et al. (2019) further identified alkanals (C_{10}-C_{14}), alkan-2-ones (C_{10}-C_{18}) and alkan-3-ones (C_{10}-C_{16}) sampled during the London Campaign, 2017. Average concentrations of grouped compounds appear in Table S1, and of specific compounds in Table S2. Figure 2 shows the organic compound composition, expressed as the relative abundance in total mass concentration (sum of gas and particle phase) collected at MR and RU. Acyclic alkanes (57%) are the most abundant hydrocarbons followed by monocyclic alkanes (17%) and monocyclic aromatics (16%) at RU. At MR, acyclic alkanes were still dominant but dropped to 36% as there was a greater contribution from monocyclic alkanes (24%), bicyclic alkanes (15%) and monocyclic aromatics (18%). Isaacman et al. (2012) reported that the diesel fuel which they analysed consisted of 73% aliphatic hydrocarbons and 27% aromatics. Alkanes accounted for nearly half (41%) of the observed mass fraction of diesel fuel, followed by 14% cycloalkanes, 11% bicyclic alkanes and 6% benzenes (Isaacman et al., 2012), broadly consistent with our own analyses (Alam et al., 2018). SVOCs (above C_{20}) emitted from gasoline and diesel-powered engines derive mainly from engine oil (Drozd et al., 2019; Alam et al., 2016b). Studies of the contribution of different components in engine lubricating oil have reported that the most abundant groups are straight, branched and cyclic alkanes (≥80%) with the largest contribution from cycloalkanes (≥27%) (Worton et al., 2014; Sakurai et al., 2003). The chemical composition of diesel fuel and lubricating oil in the literature well explain the overwhelming presence of acyclic alkanes, monocyclic alkanes and bicyclic alkanes in the urban air samples.

The carbon distribution of I/SVOCs in Figure 2 is in broad agreement with the carbon distribution of diesel fuel reported by Gentner et al. (2012), who demonstrated a sharp peak at around C_{10} to C_{13} and a broader peak at around C_{16}-C_{20}. A correlation analysis was carried out between the I/SVOCs measured in the London air and diluted emissions from a light-duty diesel engine designed to a Euro 5 standard under three different operation modes (low-speed/low-load, high-speed/low-load and high-speed/high load), without or with aftertreatment by a diesel oxidation catalyst (DOC) and diesel particulate filter (DPF) (Alam et al., 2019). Total I/SVOCs (sum of acyclic alkanes, cyclic alkanes and aromatics in the gas phase and particle phase) ranging from C_{13} to C_{36} collected at MR and RU correlated strongly with the diesel exhaust (Table S3), indicating that the I/SVOCs measured in London air have a similar carbon distribution and composition as those measured in the diesel exhaust. The I/SVOCs at the roadside site MR (r^2=0.71-0.81) generally correlated better with the diesel exhaust than those sampled at the background site RU (r^2=0.56-0.76). The on-road light-duty diesel fleet includes older vehicles without abatement devices, vehicles with only DOC, and vehicles with both a DOC and DPF (Alam et al., 2019). The correlation between I/SVOCs in London air and diesel exhaust emitted under different operation conditions without or with aftertreatment varies little. Compounds observed in the gas phase of diesel emissions are similar to those identified in diesel fuels (mainly below C_{20}) while compounds in the particle phase are similar to lubricating oil (mainly C_{21}-C_{27}) (Alam et al., 2018). The similarities found in the I/SVOC profiles in urban air and diesel exhaust clearly demonstrate the impact of diesel-powered vehicles upon urban air quality.

While London has a high percentage of diesel vehicles, it is likely that there are other sources of I/SVOCs that are contributing to urban air besides diesel- exhaust. The majority of IVOCs emitted from gasoline engines have volatility similar to C_{12}-C_{14} n-alkanes and comprise aliphatic and aromatic compounds with published work reporting a large fraction of unspeciated UCM (Drozd et al., 2019; Zhao et al., 2016). I/SVOCs below C_{18} measured at MR correlated more strongly with the

gasoline-tracer benzene (r^2=0.46-0.71) rather than those above C_{18} (r^2=0.005-0.10), indicating a substantial gasoline emission contribution to the more volatile organics. Some organic markers (i.e. n-alkanes and PAHs) have been detected in on-road non-exhaust emissions, such as from tyre and brake lining wear and in road dust (Rogge et al., 1993; Pant and Harrison, 2013; Kwon and Castaldi, 2012; El Haddad et al., 2009). The use of volatile chemical products (VCPs) (e.g. pesticides, coating, cleaning and personal care products) can contribute to urban organic emissions, and that mineral spirits commonly used in solvent-borne coatings can be a source of nonoxygenated IVOCs (McDonald et al., 2018).Khare and Gentner (2018) suggest that asphalt-related road paving and repair could also be a source of I/SVOCs. Aliphatic and aromatic VOCs and IVOCs up to C_{18}, with minor SVOCs present, were detected in paving-related products. During the paving processes (i.e. hot storage, application and surfacing), the degradation of larger organic compounds in heated asphalts can generate lighter compounds ranging from C_7 to C_{30}, such as alkanes, cyclic alkanes and single-ring aromatics that may also contribute to the I/SVOC roadside concentrations due to their long emission timescales after application.

3.1.2 Acyclic alkanes

Figure 3 shows the split between gas and particle concentrations for the I/SVOC classes. Alkane homologues including linear n-alkanes and branched alkanes were grouped depending on their carbon number. Alkanes from C_{13} to C_{31} were detected in both the particulate and gas phase while C_{32} to C_{36} were detected only in the particulate phase. A number of studies have distinguished the origin of n-alkanes by applying the carbon preference index (CPI), calculated by the summation of odd carbon number n-alkanes over a carbon range divided by the summation of even carbon number n-alkanes over the same carbon range (Cincinelli et al., 2007; Andreou and Rapsomanikis, 2009; Simoneit, 1999). The I/SVOCs emitted from natural sources (e.g. plant wax) present CPI >1 while from fossil fuel sources (e.g. vehicle emission) present CPI close to or lower than 1

(Simoneit, 1999). The CPI values for alkanes at RU (average CPI=1.13) and MR (average CPI=1.05) indicate an origin mainly from fossil fuel sources, such as vehicle emissions, and are discussed in more depth in a companion paper (Xu et al., 2020.

The distribution of the acyclic alkanes in Figure 3 has been correlated with diesel engine emissions and is similar to that reported for gas-phase (r^2=0.64 at MR; r^2=0.56 at RU) and particle-phase diesel exhaust (r^2=0.64 at MR; r^2=0.42 at RU) measured by Alam et al.(2019), showing diesel exhaust is the potential emission source for acyclic alkanes, in agreement with the CPI results. The distribution of alkanes shown in Figure 3 bears a strong similarity to that for n-alkanes reported from Delhi by Gupta et al. (2017), but differs from measurements in Guangzhou (Bi et al., 2003) and Athens (Mandalakis et al., 2002) which lack the mode at lower carbon numbers, presumably because of a lower abundance of diesel vehicles. A larger mode at lower carbon numbers in this study might also due to the lighter and more volatile hydrocarbons found in gasoline emissions.

3.1.3 Monocyclic alkanes and bicyclic alkanes

In most previous studies, the mixture of cyclic alkanes and branched alkanes has typically been observed as a part of the unresolved complex mixture (UCM) (Mandalakis et al., 2002) or classified as groups of compounds (Dunmore et al., 2015). This study has separated the monocyclic alkane and bicyclic alkane components (structure of chemicals shown as Figure S5-S6) from UCM based on their retention behaviour in the 2D chromatography.

Monocyclic alkanes ranging from C_{12} to C_{18} were detected in the particulate and gas phases while C_{19} to C_{25} were detected only in the particle phase (Figure 3). Alkyl-cyclopentane, alkyl-cyclohexane and alkyl-cycloheptane and their derivatives were observed in the monocyclic alkane groups. Alkenes were observed but not well separated from the monocyclic alkane polygons. The

observed alkenes had very low concentrations, consistent with the finding of Gentner et al. (2012), so that the influence of alkenes on the group concentration was estimated as negligible. Bicyclic alkanes ranging from C_{13} to C_{17} were detected in the particulate and gas phases while C_{18} to C_{27} were detected only in the particle phase (Figure 3). Isaacman et al. (2012) reported the semi-volatile organic compound composition of diesel fuel, and cycloalkanes accounted for a more significant fraction of diesel fuel (14%) than bicyclic alkanes (11%), broadly consistent with the air samples. Alkyl-cyclohexanes from C_{12} to C_{25} were also quantified in this study and shown in Table S2. Concentrations of alkyl-cyclohexanes presented similar patterns to those for grouped monocyclic alkanes in Figure 3 and on average accounted for around 30% of the monocyclic alkane groups.

3.1.4 Monocyclic aromatics

Approximately 30% of gasoline mass and 20% of diesel fuel mass are aromatics while the remaining components are comprised largely of alkane classes (acyclic and cyclic) (Gentner et al., 2013). Monocyclic aromatics ranging from C_{10} to C_{19} were detected in the particulate and gas phase air samples while C_{20} to C_{24} were detected only in the particle phase. Monocyclic aromatic homologues occupied the third largest percentage of the total chemicals (18% at MR and 16% RU).. The C_{10} homologue was the most abundant in the gas phase with a further peak at C_{15} while the particle phase distribution was steady throughout C_{10} to C_{19} with an increase for C_{19} and above (Figure 3). Monocyclic aromatics ranging from C_{10} to C_{11} represent a large fraction of the IVOC emission of gasoline exhaust (Drozd et al., 2019), suggesting that the light monocyclic aromatics in the gas phase may derive from both gasoline and diesel-powered vehicles.

3.2 The Influence of Wind Direction

The air flow within a street canyon is strongly influenced by street orientation and the wind conditions. Wind direction is the most important factor affecting the flow and mixing processes in the street canyon and the consequent I/SVOC concentrations (arising from emissions within the

street canyon) (Kumar et al., 2008). The MR sampling site is at the kerbside on the southern side of the heavily trafficked Marylebone Road, which is relatively straight and oriented in the west–east direction. The buildings on either side of Marylebone Road are around six storeys in height giving a street canyon aspect ratio of approximately 1:1 (Harrison et al., 2019). Typically, winds can set up a single vortex in a regular street canyon (aspect ratio ~1) when the wind is across the canyon (wind direction to the street axis exceeds 30°) with a wind speed above 1.5 m s^{-1} (Kumar et al., 2008; DePaul and Sheih, 1985).

There were 25 daily samples collected at MR, including eight south wind days, six north wind days and 11 mixed flow days. The average concentrations of the main I/SVOC groups during the north wind and south wind have been calculated and compared (Figure 4). In a street canyon, air exchange between the street level and the atmosphere on the rooftop level is limited. The traffic emitted pollutants in the street are less diluted due to the buildings at the roadside, especially in winter as a result of a more stable weather conditions (Wehner et al., 2002; Gromke et al., 2008). A schematic diagram from our previous work of the wind flows in the street canyon of Marylebone Road shows how southerly winds and northerly winds transport the pollutants from Marylebone Road to MR and WM monitoring sites respectively (Harrison et al., 2019). During the south wind, the sampler at the southern side of Marylebone Road was heavily exposed to the freshly emitted traffic pollutants from the road. During the north wind, the MR sampler was exposed mainly to incoming air from the background atmosphere of north London, resulting in a reduced concentration of I/SVOCs compared to the average concentrations of the entire campaign. This is seen clearly for alkanes (n+i) in Figure 4, and shows that the hydrocarbon distribution in background north London air is very similar to that in the air heavily polluted by vehicle emissions when the wind is in the southerly sector (r^2=0.90)

3.3 Spatial Distribution of Concentrations

Samples were collected at WM and RU simultaneously from 24 January to 19 February 2017, and after that MR sampling was run from 22 March to 18th April 2017. The difference of sampling period makes comparability between these sites more difficult. The concentrations of organic compounds are typically higher in winter than in summer, attributed to the differences in meteorological parameters as well as the strength of seasonal particulate emissions, such as from residential heating, and lower breakdown rates. SOA formation from urban emissions in winter can be as efficient as the SOA production observed in summer (Schroder et al., 2018). The significant variation in seasonal concentrations of particulate matter has been reported in several studies (Fu et al., 2008; Pant et al., 2015; Singh et al., 2011; Yadav et al., 2013.

In order to better understand the spatial distribution of I/SVOCs, scaling of the MR I/SVOC concentrations was applied to estimate the I/SVOC concentrations as if MR had been sampled simultaneously with WM/RU (January-February 2017) by taking account of BC as a dispersion marker. In London, BC arises very largely from vehicle traffic (Harrison and Beddows, 2017; Harrison et al., 2019) and the major fraction of BC measured at the roadside site MR comes from traffic emissions. The sum of I/SVOCs in the gas phase and particle phase correlated moderately with BC at MR during the MR campaign period (average r^2=0.40) below C_{28} while there was a weaker correlation for I/SVOCs above C_{28} (average r^2=0.20). I/SVOCs at MR during the WM/RU sampling campaign were estimated based on the original MR I/SVOC concentrations multiplied by the ratio of MR BC during the WM/RU sampling period to that during the MR sampling period (estimation details in Supplementary Information Section 5). The concentrations of alkanes, monocyclic alkanes, bicyclic alkanes and monocyclic aromatics at WM and RU during January to February 2017 and scaled data from MR (sum of the gas phase and particle phase) are shown in Figure 5. Expectedly, MR concentrations were the highest of all sites as it is a heavily trafficked site. The concentrations of hydrocarbons at WM were higher than RU presumably reflecting a

410 greater distance of RU from the source of emissions. The carbon distribution of these I/SVOC
411 groups presented in Figure 5 was similar at the three sampling sites and presented $r^2 \geq 0.58$ (Table
412 S4), implying the dispersion of traffic emission to the downwind area. While traffic, especially
413 diesel emissions, was suggested as the dominant emission sources for the I/SVOCs identified in the
414 current study, small differences between sites indicate the likely presence of other sources, such as
415 roadside dusts and the use of VCP.
416
417 Results in the current study were compared with a recent gas-phase I/SVOC study (Dunmore et al.,
418 2015) at North Kensington (NK) in London, which is classified as an urban background site by the
419 UK automatic air quality network (Dall'Osto et al., 2011). Dunmore et al. (2015) grouped alkanes,
420 alkenes and cycloalkanes as aliphatic compounds, suggesting approximately 5600 ng/m^3 for C_{13} in
421 January/February. To compare with the NK study (Dunmore et al., 2015), gas phase concentrations
422 of the alkane groups and monocyclic alkane groups in MR during January-February were summed,
423 reporting a very much lower concentration for C_{13} (282 ng/m^3). The degree of traffic pollution, as
424 represented by the BC concentration was however higher in the Dunmore et al. (2015) study.
425
426 **3.4 Estimation of the Emission Factors (EFs) of I/SVOCs Detected at MR**
427 MR is a congested urban street canyon where vehicle speeds vary greatly over short distances
428 (Jones and Harrison, 2006) and the traffic flow is over 80,000 vehicles per day. Jones and Harrison
429 (2006) estimated the fleet-average emission factors (EFs) of NO_x at Marylebone Road (MR) in
430 2002/2003 based on the fleet composition and traffic emissions from the National Atmospheric
431 Emissions Inventory (NAEI) database. The NO_x EF at MR during the MR campaign 2017 was
432 estimated by scaling the NO_x EF in 2002/2003 reported by Jones and Harrison (2006) by the ratio
433 of NO_x concentrations (minus background) in the two periods accounting also for the traffic mix
434 and flows. The roadside increments ($PM_{2.5}$, $PM_{2.5-10}$, PM_{10}) correlated most strongly with roadside
435 NO_x, which is frequently used as a dispersion tracer (Jones and Harrison, 2006). The EFs of

436 I/SVOC groups were estimated based on the assumption that the I/SVOCs and NO_x in the traffic
437 increments (minus background) come from the common traffic source and disperse similarly in the
438 ambient air, enabling the EFs of I/SVOC to be estimated from the ratio of their concentrations to
439 those of NO_x (minus background) (see Supplementary Information, Section 6). A number of
440 previous studies have applied this method (Johansson et al., 2009; Ketzel et al., 2003; Omstedt et
441 al., 2005; Wåhlin et al., 2006) or assumption (Gietl et al., 2010; Gidhagen et al., 2005) to estimate
442 the EFs of pollutants.
443
444 The emission factor of NO_x on Marylebone Road for the mixed fleet was estimated as 0.82 g (NO_x
445 as NO_2) veh^{-1} km^{-1}, based upon the mean concentrations during the MR sampling period. A major
446 change in the fleet composition between the early 2000s and the present day is that the proportion
447 of diesel-powered light-duty vehicles (LDVs) has grown. The numbers of gasoline-powered LDVs
448 and diesel-powered LDVs are similar in the UK currently while most of the heavy-duty vehicles
449 (HDVs) in Europe are diesel-powered (Carslaw et al., 2011; Hassler et al., 2016). Diesels contribute
450 the majority of burned fuel for transportation in the UK (Dunmore et al., 2015). Since only the
451 gasoline-powered vehicles have shown a remarkable reduction in NO_x emissions in the past two
452 decades, and the NO_x emission from diesel vehicles have not declined much during the same time
453 period (Carslaw and Rhys-Tyler, 2013), the roadside NO_x emission have remained stable in the UK
454 (Carslaw et al., 2011; Hassler et al., 2016) Carslaw et al. (2011) reported that the NO_x EFs were
455 variable based on different estimates. The UK NAEI assumes a much lower proportion of Euro
456 1/Euro 2 for petrol vehicles than that suggested by RSD (remote sensing detector) and does not
457 differentiate the age of vehicles by area/road type (e.g. urban area and motorways). The differences
458 in the fleet composition and vehicle age assumed in the NAEI and observed by RSD are important
459 factors affecting the NOx emission estimates.
460

Four main classes of compounds, including alkanes, monocyclic alkanes, bicyclic alkanes and monocyclic aromatics, accounted for 92% of the gas phase and 99.5% of the particle phase identified emissions. Emission factors of the four main I/SVOC groups by carbon number and phase appear in Figure 6. Particle phase alkanes (n+i) had the highest total emission factor among all particle phase compound classes in this study while the emissions of monocyclic alkanes, bicyclic alkanes, monocyclic aromatics and naphthalene were more abundant in the gas phase than in the particle phase.

The n-alkane emission factors estimated in this study are shown in Table S7 and compared with several previous roadside studies and lab tests although the comparisons between EFs measured under different conditions is not straightforward The three roadside studies are the Zhujiang Tunnel study in China (He et al., 2008), the roadside study of Route 467 in Fujisawa, Japan (Kawashima et al., 2006) and the roadside study of Grenoble Ring Road in Grenoble, France (Charron et al., 2019). The background information on these studies can be seen in Table S8, including sampling date, vehicle speed, traffic volume and the proportion of light duty vehicles (LDVs) and heavy-duty vehicles (HDVs). The emission factors of n-alkanes measured in the gas phase in this study were markedly lower than in the roadside study in Japan (Kawashima et al., 2006), while the emission factors of particle phase n-alkanes ranging from C_{19}-C_{26} showed a broad agreement with the tunnel study in China (He et al., 2008) and the roadside study in France (Charron et al., 2019), all of which showed a similar order of magnitude and a broad peak at around C_{21}-C_{25}. Greater particle-phase emissions of long chain n-alkanes (above C_{27}) were detected in this study compared with the Zhujiang Tunnel study in China (He et al., 2008).

Vehicle fleet composition varies appreciably between countries. There are far fewer light duty diesel powered vehicles in China and Japan than in the EU. Gasoline engines are typically used in light-duty vehicles (LDVs) in these former countries whilst diesel engines dominate in heavy-duty

vehicles (HDVs). There has been a significant shift to diesel engines in the small vehicle market in recent years, especially in several European countries (EMEP/EEA, 2016). Diesel vehicles represented 40% of the vehicles in 2017 in the UK (Fleet News, 2018) while accounting for 72% of vehicles in 2011 in France (Charron et al., 2019). In contrast, light duty gasoline vehicles represent a large percentage of the Chinese vehicle fleet and the share increased rapidly from less than 50% in 2002 to 70% in 2009 (Huo et al., 2012). In Japan, the ratio of diesel-powered small trucks to gasoline powered vehicles is 8.1% (Kawashima et al., 2006). Gentner et al. (2012) measured the carbon distribution of straight and branched chain alkanes from gasoline and diesel-powered vehicles, finding a predominant contribution of gasoline combustion to the lighter alkanes (up to C_{12}). Diesel emissions are mainly comprised of heavier aliphatic hydrocarbons containing primarily unburned fuel (up to C_{20}) and unburned lubricating oil (C_{18} to C_{36}) (Alam et al., 2016a). Therefore, greater emissions of light alkanes might be expected in the gas phase in Japan as gasoline powered vehicles dominate the market. The composition of lubricants may explain the difference in the long chain n-alkane (above C_{27}) emissions in this study and the Zhujiang Tunnel study in China (He et al., 2008). The differences of the EFs in these studies are probably mainly caused by variations in the vehicle type and the composition of fuel/oil in use, as well as the road conditions and vehicle speed.

Also included in Table S7 are the emission factors for particle-phase hydrocarbons measured by chassis dynamometer tests for diesel-powered passenger cars of Euro 2, Euro 3, Euro 4, and Euro 4 with a particle trap (Charron et al., 2019; Perrone et al., 2014). Perrone et al. (2014) reported the n-alkane EFs from Euro 2 decreased to one-fifth of Euro 1, and declined further to Euro 3, indicating the n-alkane EFs have a strong association with the technological development of the LDVs. The fleet average on-road emission factors measured both in this work and by Charron et al. (2019) in Table S7 generally exceed the values for Euro 3 vehicles (Charron et al., 2019; Perrone et al., 2014) but are closer to Euro 2 without an emission control device (Perrone et al, 2014), despite the fact

that most vehicles would have been built to more recent Euro standards at the time of sampling, and many would be fitted with a diesel particle filter (DPF). This suggests a major contribution from the heavy-duty vehicles and/or many high emission vehicles with malfunctions in their emissions control devices, or an unrepresentative test cycle in the laboratory work.

The C_{20}-C_{32} n-alkane EF profiles detected in the particle-phase of diesel emissions show a maximum n-alkane EF at C_{20}-C_{22} and a decrease in EF with the increase of carbon number (Charron et al., 2019; Perrone et al., 2014). Past studies have reported a similar profile of n-alkane EFs in diesel exhaust of medium-duty trucks (Schauer et al., 1999), heavy-duty vehicles (Shah et al., 2005) and Euro 4 vehicle tested for the urban cycle with cold start (Kim et al., 2016). The difference between the n-alkane EFs from the ambient air of London roadside and the laboratory measurements of diesel-powered vehicles may be attributed to the presence of other emission sources in London air, such as the exhaust from gasoline-powered vehicles and non-exhaust sources (e.g. asphalt-related paving). The carbon number distribution of n-alkane EFs in the particle phase can also be affected by dilution ratio (DR) which may differ from the laboratory tests (typically lower DR) to measurements in ambient air (higher DR) (Perrone et al, 2014). Fujitani et al. (2012) reported that the distribution of n-alkane EFs ranging from C_{12} to C_{33} between the gas phase and particle phase in diesel exhaust varied with DR, since the gas-particle partitioning depends strongly on DR and vapour pressure.

4. OVERVIEW

The comparisons between the composition and carbon number distribution of I/SVOCs in urban air samples with those of diesel exhaust show high similarities, indicating the diesel exhaust is the most probable source of the species identified in this study. Besides diesel fuel, the potential of other emission sources of I/SVOCs in urban air have been discussed, such as gasoline engine emissions, tyre and brake lining wear, the use of volatile chemical products (VCPs) and asphalt-related paving.

The lower molecular weight C_{13} to C_{18} hydrocarbons were primarily in the gas phase, while the hydrocarbons above C_{20} were more abundant in the particulate phase. The peak abundance of hydrocarbons of C_{10}-C_{20} is attributed to diesel fuel, and those of C_{21}-C_{28} largely to engine oil. As expected, concentrations at MR were the highest of all sites as it is a heavily trafficked roadside. The concentration of hydrocarbons at WM was higher than RU as the emissions were diluted more at an increased distance from the traffic emission source. The alkane concentrations at MR were highest when the south wind brought the traffic emitted pollutants to the MR sampler, while concentrations were lowest when the north wind brought background air from north London.

Emission factors have been estimated and four classes of compounds, including alkanes (n+i), monocyclic alkanes, bicyclic alkanes and monocyclic aromatics made a dominant contribution to emissions at MR. Although it is a challenge to compare directly the emission factor with other studies conducted under different conditions, the emission factors of n-alkanes estimated in the current study showed a similar order of magnitude and broad agreement with the tunnel study in China (He et al., 2008) and the roadside study in France (Charron et al., 2019). The gas-phase n-alkanes in a roadside study in Japan (Kawashima et al., 2006) were significantly higher than in this study, probably caused by variations in the vehicle type and the composition of fuel/oil in use, as well as the road conditions and vehicle speed. The comparison between the n-alkane EFs estimated in the current study and those measured directly in diesel exhaust indicate a considerable contribution from vehicles with higher emissions than recent diesel passenger cars to London air. Differences in the n-alkane profiles between London air and diesel exhaust may be attributed to a number of factors, such as the presence of gasoline emissions and different dilution ratios (DRs) in real world measurements and lab tests.

DATA ACCESSIBILITY

Data supporting this publication are openly available from the UBIRA eData repository at https://doi.org/10.25500/edata.bham.00000310.

ACKNOWLEDGEMENTS

The authors acknowledge funding from the European Research Council for the FASTER project (ERC-2012-AdG, Proposal No. 320821). The authors acknowledge Dr David Beddows and Dr Ajit Singh for their help during sampling campaigns.

SUPPORTING INFORMATION

Supporting Information provides further details of sampling site locations, the 24-hour air sampler, the analysis of 2-D-chromatograms, the specific compound analyses, and the estimation of emission factors.

CONFLICT OF INTERESTS

The authors declare no competing financial interest.

583 **REFERENCE**

584

585 Alam, M.S., Zeraati-Rezaei, S., Xu, H., Harrison, R.M., 2019. Characterisation of gas and
586 particulate phase organic emissions (C_9-C_{37}) from a diesel engine and the effect of abatement
587 devices, Environ. Sci. Technol., 53, 11345-11352.
588
589 Alam, M.S., Liang, Z., Zeraati-Rezaei, S., Stark, C., Xu, H., MacKenzie, A.R, Harrison, R.M.,
590 2018. Mapping and quantifying isomer sets of hydrocarbons (≥C12) in diesel exhaust, lubricating
591 oil and diesel fuel samples using GC×GC-ToFMS. Atmos. Meas. Techn., 11, 3047-3058.
592
593 Alam, M.S., Harrison, R.M., 2016. Recent advances in the application of 2-dimensional gas
594 chromatography with soft and hard ionisation time-of-flight mass spectrometry in environmental
595 analysis. Chem. Sci., 7, 3968-3977.
596
597 Alam, M.S., Zeraati-Rezaei, S., Stark, C.P., Liang, Z., Xu, H., Harrison, R.M., 2016a. The
598 characterisation of diesel exhaust particles–composition, size distribution and partitioning. Faraday
599 Discuss., 189, 69-84.
600
601 Alam, M.S., Stark, C., Harrison, R.M., 2016b. Using variable ionisation energy time-of-flight mass
602 spectrometry with comprehensive GC×GC to identify isomeric species. Anal. Chem., 88, 4211-
603 4220.
604
605 Andreou, G., Rapsomanikis, S. 2009. Origins of n-alkanes, carbonyl compounds and molecular
606 biomarkers in atmospheric fine and coarse particles of Athens, Greece. Sci. Total Environ., 407**,**
607 5750-5760.
608
609 Bi, X., Sheng, G., Peng, P., Chen, Y., Zhang, Z., Fu, J., 2003. Distribution of particulate- and
610 vapor-phase n-alkanes and polycyclic aromatic hydrocarbons in urban atmosphere of Guangzhou,
611 China. Atmos. Environ., 37, 289-298.
612
613 Carslaw, D. C. and Rhys-Tyler, G., 2013. New insights from comprehensive on-road measurements
614 of NO_x, NO_2 and NH_3 from vehicle emission remote sensing in London, UK. Atmos. Environ., 81,
615 339-347.
616
617 Carslaw, D.C., Beevers, S.D., Tate, J.E., Westmoreland, E.J., Williams, M. L. 2011. Recent evidence
618 concerning higher NOx emissions from passenger cars and light duty vehicles. Atmos. Environ., 45,
619 7053-7063.
620
621 Chan, A.W.H., Isaacman, G., Wilson, K.R., Worton, D.R., Ruehl, C.R., Nah, T., Gentner, D.R.,
622 Dallmann, T.R., Kirchstetter, T.W., Harley, R.A., Gilman, J.B., Kuster, W.C., De Gouw, J.A.,
623 Offenberg, J.H., Kleindienst, T.E., Lin, Y.H., Rubitschun, C.L., Surratt, J.D., Hayes, P.L., Jimenez,
624 J.L., Goldstein, A.H. 2013. Detailed chemical characterization of unresolved complex mixtures in
625 atmospheric organics: Insights into emission sources, atmospheric processing, and secondary
626 organic aerosol formation. J. Geophys. Res.: Atmospheres, 118, 6783-6796.
627
628 Charron, A., Polo-Rehn, L., Besombes, J.-L., Golly, B., Buisson, C., Chanut, H., Marchand, N.,
629 Guillaud, G., Jaffrezo, J.-L., 2019. Identification and quantification of particulate tracers of exhaust
630 and non-exhaust vehicle emissions. Atmos. Chem. Phys., 19, 5187-5207, 2019.
631
632 Cincinelli, A., Bubba, M. D., Martellini, T., Gambaro, A., Lepri, L. 2007. Gas-particle concentration
633 and distribution of n-alkanes and polycyclic aromatic hydrocarbons in the atmosphere of Prato
634 (Italy). Chemosphere, 68, 472-8.

Dall'Osto, M., Thorpe, A., Beddows, D.C.S., Harrison, R.M., Barlow, J.F., Dunbar, T., Williams, P.I., Coe, H., 2011. Remarkable dynamics of nanoparticles in the urban atmosphere. Atmos. Chem. Phys., 11, 6623-6637.

DePaul, F., Sheih, C., 1985. A tracer study of dispersion in an urban street canyon. Atmos. Environ., 19, 555-559.

Donahue, N.M., Kroll, J., Pandis, S.N., Robinson, A.L. 2012. A two-dimensional volatility basis set–Part 2: Diagnostics of organic-aerosol evolution. Atmos. Chem. Phys., 12, 615-634.

Drozd, G. T., Zhao, Y., Saliba, G., Frodin, B., Maddox, C., Oliver Chang, M. C., Maldonado, H., Sardar, S., Weber, R. J., Robinson, A. L. & Goldstein, A. H. 2019. Detailed speciation of intermediate volatility and semivolatile organic compound emissions from gasoline vehicles: Effects of cold-starts and implications for secondary organic aerosol formation. Environ Sci Technol, 53, 1706-1714.

Duffy, B.L., Nelson, P.F. 1996. Non-methane exhaust composition in the Sydney Harbour Tunnel: A focus on benzene and 1, 3-butadiene. Atmos. Environ., 30**,** 2759-2768.

Dunmore, R., Hopkins, J., Lidster, R., Lee, J., Evans, M., Rickard, A., Lewis, A., Hamilton, J., 2015. Diesel-related hydrocarbons can dominate gas phase reactive carbon in megacities. Atmos.Chem. Phys., 15, 9983-9996.

El Haddad, I., Marchand, N., Dron, J., Temime-Roussel, B., Quivet, E., Wortham, H., Jaffrezo, J.L., Baduel, C., Voisin, D., Besombes, J.L., 2009. Comprehensive primary particulate organic characterization of vehicular exhaust emissions in France. Atmos. Environ., 43, 6190-6198.

EMEP/EEA, 2016. Air Pollutant Emission Inventory Guidebook 2016, Technical guidance to prepare national emission inventories. EEA Report No. 21/016, European Environment Agency, Denmark, 2016, file:///C:/Users/hardinmt/Downloads/EMEP%20EEA%20air%20pollutant%20emission%20inventory%20guidebook%202016%20Introduction%20(3).pdf [last accessed 18 October 2019].

Fleet News, 2018. Record number of diesel cars now on Britain's roads, says RAC Foundation, https://www.fleetnews.co.uk/news/manufacturer-news/2018/04/16/diesel-cars-reach-record-number-in-britain [last accessed 07/02/2019].

Frysinger, G.S., Gaines, R.B., Xu, L., Reddy, C.M., 2003. Resolving the unresolved complex mixture in petroleum-contaminated sediments. Environ. Sci. Tecnol., 37, 1653-1662.

Fu, P., Kawamura, K., Barrie, L. A., 2008. Photochemical and other sources of organic compounds in the Canadian high Arctic aerosol pollution during winter-spring. Environ. Sci. Technol., 43, 286-292.

Fujitani, Y., Saitoh, K., Fushimi, A., Takahashi, K., Hasegawa, S., Tanabe, K., Kobayashi, S., Furuyama, A., Hirano, S., Takami, A., 2012. Effect of isothermal dilution on emission factors of organic carbon and n-alkanes in the particle and gas phases of diesel exhaust. Atmos. Environ., 59, 389-397.

Gentner, D.R., Worton, D.R., Isaacman, G., Davis, L.C., Dallmann, T.R., Wood, E.C., Herndon, S.C., Goldstein, A.H., Harley, R.A. 2013. Chemical composition of gas-phase organic carbon emissions from motor vehicles and implications for ozone production. Environ. Sci. Technol., 47, 11837-11848.

Gentner, D.R., Isaacman, G., Worton, D.R., Chan, A.W., Dallmann, T.R., Davis, L., Liu, S., Day, D.A., Russell, L.M., Wilson, K.R., 2012. Elucidating secondary organic aerosol from diesel and gasoline vehicles through detailed characterization of organic carbon emissions. Proc. Natl. Acad. Sci., 109, 18318-18323.

Gidhagen, L., Johansson, C., Langner, J., Foltescu, V.L., 2005. Urban scale modeling of particle number concentration in Stockholm. Atmos. Environ., 39, 1711-1725.

Gietl, J.K., Lawrence, R., Thorpe, A.J., Harrison, R.M., 2010. Identification of brake wear particles and derivation of a quantitative tracer for brake dust at a major road. Atmos. Environ., 44, 141-146.

Goldstein, A.H., Galbally, I.E., 2007. Known and unexplored organic constituents in the Earth's atmosphere. Environ. Sci. Technol., 41, 1514-1521.

Gromke, C., Buccolieri, R., Di Sabatino, S., Ruck, B., 2008. Dispersion study in a street canyon with tree planting by means of wind tunnel and numerical investigations–evaluation of CFD data with experimental data. Atmos. Environ., 42, 8640-8650.

Gupta, S., Gadi, R., Mandal, T.K., 2017. Seasonal variations and source profile of n-alkanes in particulate matter (PM_{10}) at a heavy traffic site, Delhi. Environ. Monit. Assess., 189, 43.

Hamilton, J. F., Lewis, A.C. 2003. Monoaromatic complexity in urban air and gasoline assessed using comprehensive GC and fast GC-TOF/MS. Atmos. Environ., 37, 589-602.

Hamilton, J., Webb, P., Lewis, A., Hopkins, J., Smith, S., Davy, P. 2004. Partially oxidised organic components in urban aerosol using GCXGC-TOF/MS. Atmos. Chem. Phys., 4, 1279-1290.

Harrison, R.M., Beddows, D.C.S., Alam, M.S., Singh, A., Brean, J., Xu, R., Kotthaus, S. and Grimmond, S., 2019. Interpretation of particle number size distributions measured across an urban area during the FASTER campaign. Atmos. Chem. Phys., 19, 39-55.

Harrison, R.M., Beddows, D.C. 2017. Efficacy of recent emissions controls on road vehicles in Europe and implications for public health. Sci. Rep., 7**,** 1152.

Harrison, R.M., Perry, R., 1986. Handbook of Air Pollution Analysis, Second Edition, Chapman and Hall, pp. 634.

Hassler, B., McDonald, B.C., Frost, G.J., Borbon, A., Carslaw, D.C., Civerolo, K., Granier, C., Monks, P.S., Monks, S., Parrish, D.D., Pollack, I.B., Rosenlof, K.H., Ryerson, T.B., von Schneidemesser, E., Trainer, M., 2016. Analysis of long-term observations of NO_x and CO in megacities and application to constraining emissions inventories. J. Geophys. Res. Letts., 43, 9920-9930.

He, L.-Y., Hu, M., Zhang, Y.-H., Huang, X.-F., Yao, T.-T., 2008. Fine particle emissions from on-road vehicles in the Zhujiang Tunnel, China. Environ. Sci. Technol., , 42, 4461-4466.

Huo, H., Yao, Z., Zhang, Y.,Shen, X., Zhang, Q., Ding, Y., He, K., 2012. On-board measurements of emissions from light-duty gasoline vehicles in three mega-cities of China. Atmos.Environ., 49, 371-377.

Hwa, M.-Y., Hsieh, C.-C., Wu, T.-C., Chang, L.-F. W., 2002. Real-world vehicle emissions and VOCs profile in the Taipei tunnel located at Taiwan Taipei area. Atmos. Environ., 36, 1993-2002.

Isaacman, G., Wilson, K.R., Chan, A.W., Worton, D.R., Kimmel, J.R., Nah, T., Hohaus, T., Gonin, M., Kroll, J. H., Worsnop, D. R., 2012. Improved resolution of hydrocarbon structures and constitutional isomers in complex mixtures using gas chromatography-vacuum ultraviolet-mass spectrometry. Anal. Chem., 84, 2335-2342.

Jacobson, M., Kittelson, D., Watts, W., 2005. Enhanced coagulation due to evaporation and its effect on nanoparticle evolution. Environ. Sci. Technol., 39, 9486-9492.

Jathar, S.H., Miracolo, M.A., Presto, A.A., Donahue, N.M., Adams, P.J., Robinson, A.L. 2012. Modeling the formation and properties of traditional and non-traditional secondary organic aerosol: problem formulation and application to aircraft exhaust. Atmos. Chem. Phys., 12, 9025-9040.

Jimenez, J., Canagaratna, M., Donahue, N., Prevot, A., Zhang, Q., Kroll, J. H., Decarlo, P. F., Allan, J. D., Coe, H., Ng, N., 2009. Evolution of organic aerosols in the atmosphere. Science, 326, 1525-1529.

Johansson, C., Norman, M., Burman, L., 2009. Road traffic emission factors for heavy metals. Atmos. Environ., 43, 4681-4688.

Jones, A.M., Harrison, R.M., 2006. Estimation of the emission factors of particle number and mass fractions from traffic at a site where mean vehicle speeds vary over short distances. Atmos. Environ., 40, 7125-7137.

Khare, P., Gentner, D.R., 2018. Considering the future of anthropogenic gas-phase organic compound emissions and the increasing influence of non-combustion sources on urban air quality. Atmos. Chem.Phys., 18, 5391-5413.

Kawashima, H., Minami, S., Hanai, Y., Fushimi, A., 2006. Volatile organic compound emission factors from roadside measurements, Atmos. Environ., 40, 2301-2312.

Ketzel, M., Wåhlin, P., Berkowicz, R., Palmgren, F., 2003. Particle and trace gas emission factors under urban driving conditions in Copenhagen based on street and roof-level observations. Atmos. Environ., 37, 2735-2749.

Kim, Y., Sartelet, K., Seigneur, C., Charron, A., Besombes, J.-L., Jaffrezo, J.-L., Marchand, N., Polo, L., 2016. Effect of measurement protocol on organic aerosol measurements of exhaust emissions from gasoline and diesel vehicles. Atmos. Environ., 140, 176-187.

Kumar, P., Fennell, P., Britter, R., 2008. Effect of wind direction and speed on the dispersion of nucleation and accumulation mode particles in an urban street canyon. Sci. Tot. Environ., 402, 82-94.

Kwon et al., 2012

Kwon, E. E., Castaldi, M. J., 2012. Mechanistic understanding of polycyclic aromatic hydrocarbons (PAHs) from the thermal degradation of tires under various oxygen concentration atmospheres. Environ. Sci. Technol., 46, 12921-12926.

Lewis, A.C., Carslaw, N., Marriott, P.J., Kinghorn, R.M., Morrison, P., Lee, A.L., Bartle, K. D., Pilling, M.J., 2000. A larger pool of ozone-forming carbon compounds in urban atmospheres. Nature, 405, 778.

Lyu, R., Alam, M. S., Stark, C., Xu, R., Shi, Z., Feng, Y., Harrison, R. M. 2019. Aliphatic carbonyl compounds (C8-C 26) in wintertime atmospheric aerosol in London, UK. Atmos. Chem. Phys., 19, 2233-2246.

Mandalakis, M., Tsapakis, M., Tsoga, A., Stephanou, E. G., 2002. Gas-particle concentrations and distribution of aliphatic hydrocarbons, PAHs, PCBs and PCDD/Fs in the atmosphere of Athens (Greece). Atmos. Environ., 36, 4023-4035.

Manning, A.J., Nicholson, K.J., Middleton, D.R., Rafferty, S.C., 2000. Field study of wind and traffic to test a street canyon pollution model. Environ. Monitor. Assess., 60, 283-313.

Masiol, M., Hofer, A., Squizzato, S., Piazza, R., Rampazzo, G., Pavoni, B., 2012. Carcinogenic and mutagenic risk associated to airborne particle-phase polycyclic aromatic hydrocarbons: a source apportionment. Atmos. Environ., 60, 375-382.

May, A.A., Presto, A.A., Hennigan, C.J., Nguyen, N.T., Gordon, T.D., Robinson, A.L., 2013a. Gas-particle partitioning of primary organic aerosol emissions:(1) Gasoline vehicle exhaust. Atmos. Environ., 77, 128-139.

May, A.A., Presto, A.A., Hennigan, C.J., Nguyen, N.T., Gordon, T.D., Robinson, A.L., 2013b. Gas-particle partitioning of primary organic aerosol emissions:(2) Diesel vehicles. Environ. Sci. Technol., 47, 8288-8296.

McDonald, B.C., de Gouw, J.A., Gilman, J.B., Jathar, S.H., Akherati, A., Cappa, C.D., Jimenez, J.L., Lee-Taylor, J., Hayes, P.L., McKeen, S.A., Cui, Y.Y., Kim, S.-W., Gentner, D.R., Isaacman-VanWertz, G., Goldstein, A.H., Harley, R.A., Frost, G.J., Roberts, J.M., Ryerson, T.B., Trainer, M., 2018. Volatile chemical products emerging as largest petrochemical source of urban organic emissions. Science 359, 760-764.

Met Office, 2006. MIDAS: UK Hourly Weather Observation Data. NCAS British Atmospheric Data Centre [Online]. Available: http://catalogue.ceda.ac.uk/uuid/916ac4bbc46f7685ae9a5e10451bae7c [Accessed 21 March 2019].

Nelson, R.K., Kile, B.M., Plata, D.L., Sylva, S.P., Xu, L., Reddy, C.M., Gaines, R.B., Frysinger, G.S., Reichenbach, S.E., 2006. Tracking the weathering of an oil spill with comprehensive two-dimensional gas chromatography. Environ. Forensics, 7, 33-44.

Omar, N.Y. M.J., Abas, M.R.B., Rahman, N.A., Tahir, N.M., Rushdi, A.I., Simoneit, B.R.T., 2007. Levels and distributions of organic source tracers in air and roadside dust particles of Kuala Lumpur, Malaysia. Environ. Geol., 52, 1485-1500.

Omstedt, G., Bringfelt, B. & Johansson, C., 2005. A model for vehicle-induced non-tailpipe emissions of particles along Swedish roads. Atmos. Environ., 39**,** 6088-6097.

Pant, P., Shukla, A., Kohl, S. D.,Chow, J. C., Watson, J. G., Harrison, R. M., 2015. Characterization of ambient $PM_{2.5}$ at a pollution hotspot in New Delhi, India and inference of sources. Atmos. Environ., , 109, 178-189.

Pant, P., Harrison, R.M., 2013. Estimation of the contribution of road traffic emissions to particulate matter concentrations from field measurements: a review. Atmos. Environ., 77, 78-97.

Perrone, M.G., Carbone, C., Faedo, D., Ferrero, L., Maggioni, A., Sangiorgi, G., Bolzacchini, E., 2014. Exhaust emissions of polycyclic aromatic hydrocarbons, n-alkanes and phenols from vehicles coming within different European classes. Atmos. Environ., 82, 391-400.

Rissler, J., Swietlicki, E., Bengtsson, A., Boman, C., Pagels, J., Sandström, T., Blomberg, A., Löndahl, J.J., 2012. Experimental determination of deposition of diesel exhaust particles in the human respiratory tract. J. Aerosol. Sci., 48, 18-33.

Robinson, A.L., Donahue, N.M., Shrivastava, M.K., Weitkamp, E.A., Sage, A.M., Grieshop, A. P., Lane, T.E., Pierce, J.R., Pandis, S.N., 2007. Rethinking organic aerosols: Semivolatile emissions and photochemical aging. Science, 315, 1259-1262.

Rogge, W.F., Hildemann, L.M., Mazurek, M. A., Cass, G.R., Simoneit, B.R., 1993. Sources of fine organic aerosol. 3. Road dust, tire debris, and organometallic brake lining dust: roads as sources and sinks. Environ. Sic. Technol., 27, 1892-1904.

Sakurai, H., Tobias, H. J., Park, K., Zarling, D., Docherty, K. S., Kittelson, D. B., Mcmurry, P. H., Ziemann, P. J., 2003. On-line measurements of diesel nanoparticle composition and volatility. Atmos. Environ., 37, 1199-1210.

Schauer, J. J., Kleeman, M. J., Cass, G. R., Simoneit, B. R. Measurement of emissions from air pollution sources. 5., 2002. C1-C32 organic compounds from gasoline-powered motor vehicles. Environ. Sci. Technol., 36, 1169-1180.

Schauer, J.J., Kleeman, M.J., Cass, G.R., Simoneit, B.R. Measurement of emissions from air pollution sources. 2., 1999. C1 through C30 organic compounds from medium duty diesel trucks. Environ. Sci. Technol., 33, 1578-1587.

Schroder, J.C., Campuzano-Jost, P., Day, D.A., Shah, V., Larson, K., Sommers, J.M., Sullivan, A.P., Campos, T., Reeves, J.M., Hills, A., Hornbrook, R.S., Blake, N.J., Scheuer, E., Guo, H., Fibiger, D.L., McDuffie, E.E., Hayes, P.L., Weber, R.J., Dibb, J.E., Apel, E.C., Jaeglé, L., Brown, S.S., Thornton, J.A., Jimenez, J.L., 2018. Sources and Secondary Production of Organic Aerosols in the Northeastern United States during winter. J. Geophys. Res.: Atmospheres, 123, 7771-7796.

Shah, S.D., Ogunyoku, T.A., Miller, J.W., Cocker, D.R., 2005. On-Road Emission Rates Of Pah And N-Alkane Compounds From Heavy-Duty Diesel Vehicles. Environ. Sci. Tecnol., 39, 5276-5284.

Simoneit, B. R., 1999. A review of biomarker compounds as source indicators and tracers for air pollution. Environ. Sci. Pollut. Res., 6, 159-169.

Singh, D., Gadi, R., Mandal, T.K., 2011. Characterization of particulate-bound polycyclic aromatic hydrocarbons and trace metals composition of urban air in Delhi, India. Atmos. Environ., 45, 7653-7663.

Staehelin, J., Keller, C., Stahel, W., Schläpfer, K., Wunderli, S., 1998. Emission factors from road traffic from a tunnel study (Gubrist tunnel, Switzerland). Part III: Results of organic compounds, SO_2 and speciation of organic exhaust emission. Atmos. Environ., 32, 999-1009.

Van Deursen, M., Beens, J., Reijenga, J., Lipman, P., Cramers, C., Blomberg, J. J., 2000. Group-type identification of oil samples using comprehensive two-dimensional gas chromatography coupled to a time-of-flight mass spectrometer (GC× GC-TOF). J. High Resol. Chromatogr., 23, 507-510.

Ventura, G.T., Kenig, F., Reddy, C.M., Frysinger, G.S., Nelson, R.K., Van Mooy, B., Gaines, R. B., 2008. Analysis of unresolved complex mixtures of hydrocarbons extracted from Late Archean sediments by comprehensive two-dimensional gas chromatography (GC× GC). Org. Geochem., 39, 846-867.

Wehner, B., Birmili, W., Gnauk, T., Wiedensohler, A., 2002. Particle number size distributions in a street canyon and their transformation into the urban-air background: measurements and a simple model study. Atmos. Environ., 36, 2215-2223.

Weitkamp, E.A., Sage, A.M., Pierce, J.R., Donahue, N.M., Robinson, A. L. 2007. Organic aerosol formation from photochemical oxidation of diesel exhaust in a smog chamber. Environ. Sci. Technol., 41, 6969-6975.

Wåhlin, P., Berkowicz, R. & Palmgren, F., 2006. Characterisation of traffic-generated particulate matter in Copenhagen. Atmos. Environ., 40, 2151-2159.

Worton, D.R., Isaacman, G., Gentner, D.R., Dallmann, T.R., Chan, A.W., Ruehl, C., Kirchstetter, T.W., Wilson, K.R., Harley, R.A., Goldstein, A.H., 2014. Lubricating oil dominates primary organic aerosol emissions from motor vehicles. Environ. Sci. Technol., 48, 3698-3706.

Xu, R., Alam, M.S., Stark, C. and Harrison, R.M. 2020. Behaviour of traffic emitted semi-volatile and intermediate volatility organic compounds within the urban atmosphere. Science of the Total Environment, 137470.

Yadav, S., Tandon, A., Attri, A.K., 2013. Characterization of aerosol associated non-polar organic compounds using TD-GC-MS: a four year study from Delhi, India. J. Hazard. Mat., 252, 29-44.

Zhao, Y., Nguyen, N. T., Presto, A.A., Hennigan, C.J., May, A.A., Robinson, A.L., 2016. Intermediate volatility organic compound emissions from on-road gasoline vehicles and small off-road gasoline engines. Environ. Sci. Technol., 50, 4554-4563.

928 **FIGURE LEGENDS:**
929
930 **Figure 1:** Typical TD-GC×GC-ToF-MS chromatogram of a particulate-phase sample collected
931 on the roof of University of Westminster (WM) in Feb 2017, demonstrating the
932 grouping of compounds.
933
934 **Figure 2:** The I/SVOC composition (gas and particle phase) identified at MR and RU in the
935 London Campaign 2017.
936
937 **Figure 3:** Concentrations of alkanes (n+i), monocyclic alkanes, bicyclic alkanes and
938 monocyclic aromatics in the gas phase and particle phase in MR and RU, London
939 Campaign 2017.
940
941 **Figure 4:** The average alkane (n+i) concentrations in MR (sum of gas phase and particle phase)
942 during the MR campaign during southerly and northerly winds.
943
944 **Figure 5:** Concentrations of alkanes (n+i), monocyclic alkanes, bicyclic alkanes and
945 monocyclic aromatics (sum of the gas phase and particle phase) at WM and RU
946 measured simultaneously from January to February 2017, together with MR data
947 adjusted to match the same time period (see text).
948
949 **Figure 6:** Emission factors of alkanes (n+i), monocyclic alkanes, bicyclic alkanes and
950 monocyclic aromatics in the gas phase and particle phase at MR.
951
952

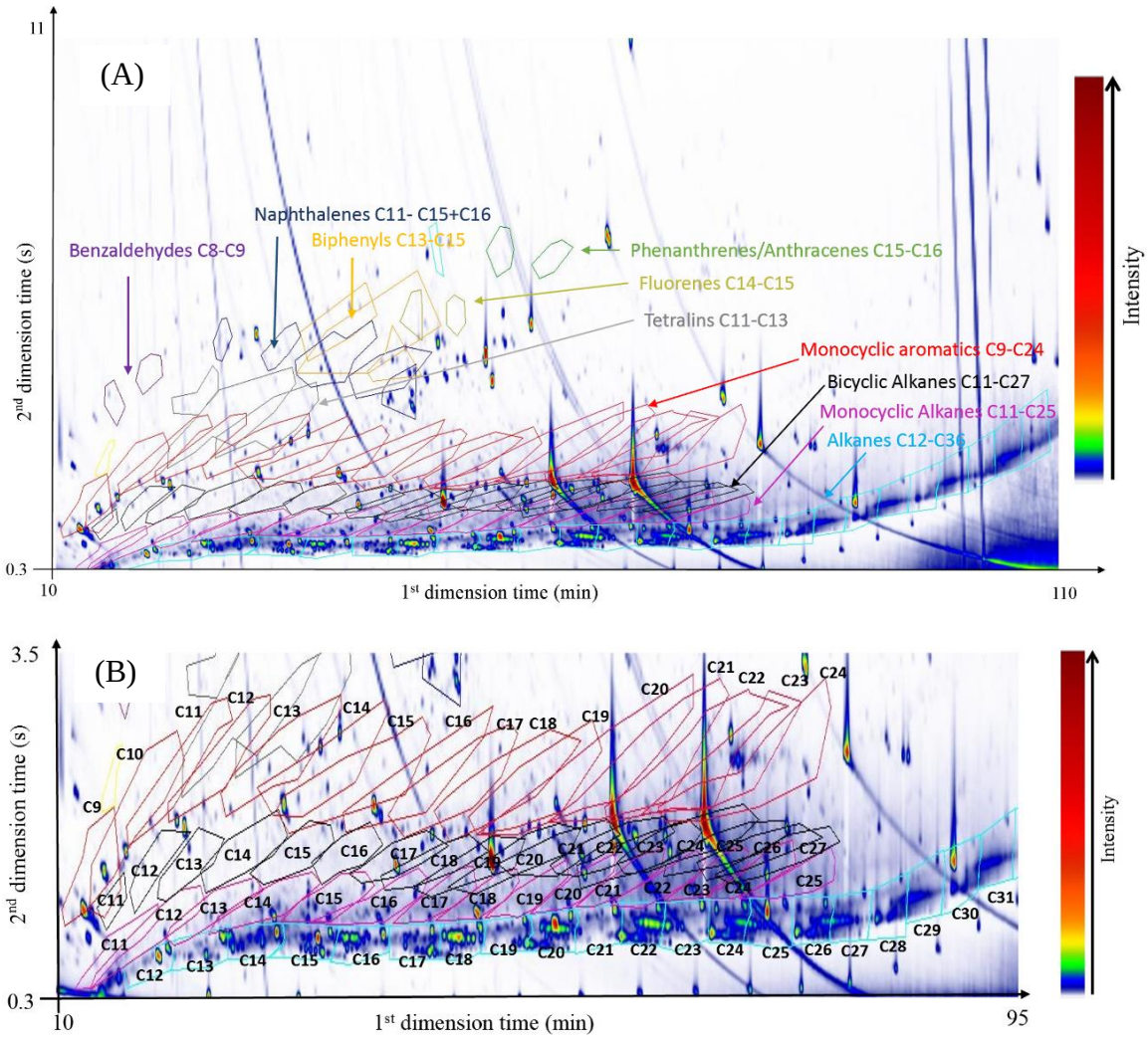

Figure 1: Typical TD-GC×GC-ToF-MS chromatogram of a particulate-phase sample collected on the roof of University of Westminster (WM) in Feb 2017, demonstrating the grouping of compounds. X and y-axis are the retention time on the first and second column respectively, with the intensity of the compounds shown by the coloured contours. Colder colours (i.e. blue) are less intense than the warmer colours (i.e. red). (A) A contour plot (chromatogram) displays C_{12}-C_{36} alkanes, C_{11}-C_{25} monocyclic alkanes, C_{11}-C_{27} bicyclic alkanes, C_9-C_{24} monocyclic aromatics, C_8-C_9 benzaldehydes, C_{11}-C_{16} naphthalenes, C_{13}-C_{15} biphenyls, C_{15}-C_{16} phenanthrenes/anthracenes, C_{14}-C_{15} fluorenes and C_{11}-C_{13} tetralins. Each region fenced by a coloured polygon marks out the grouped isomers of a chemical homologue with a particular carbon number. (B) A zoomed in contour plot displaying the carbon number distribution of grouped alkanes (blue), monocyclic alkanes (pink), bicyclic alkanes (black) and monocyclic aromatics (red).

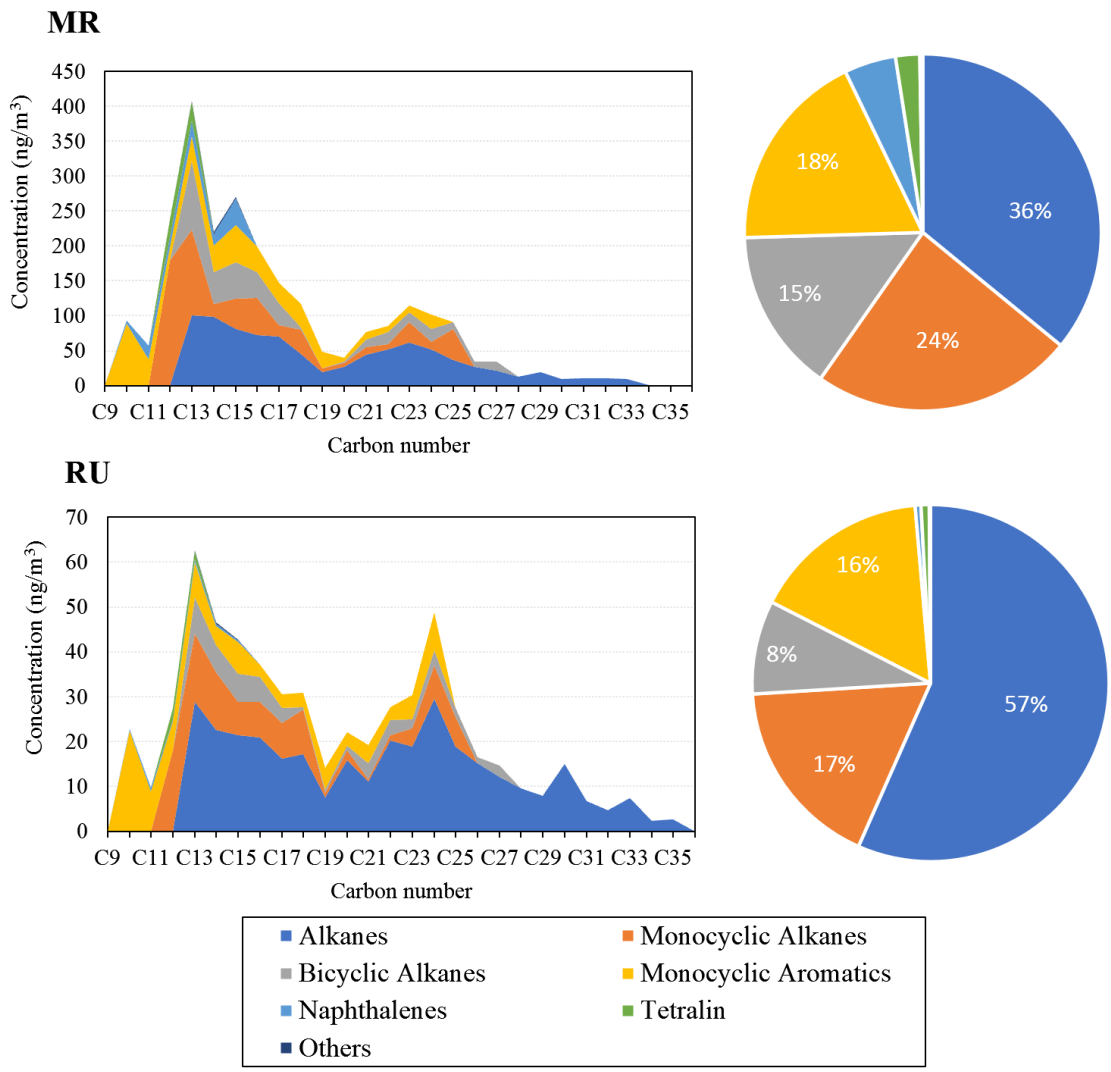

967

968 **Figure 2:** The I/SVOC composition (gas and particle phase) identified at MR and RU in the
969 London Campaign 2017.

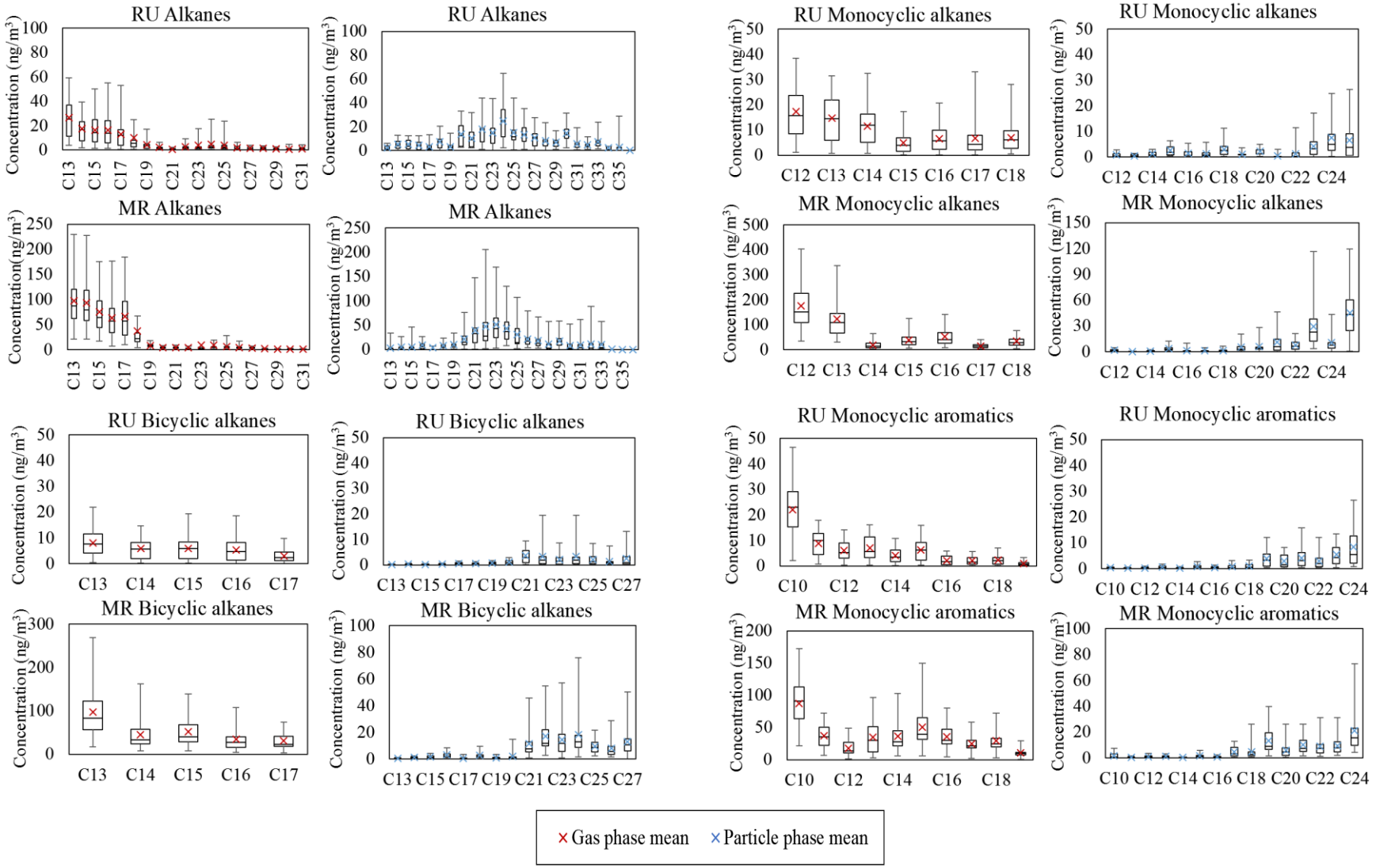

970

971

972 **Figure 3:** Concentrations of alkanes (n+i), monocyclic alkanes, bicyclic alkanes and monocyclic aromatics in the gas phase and particle phase at MR
973 and RU, London Campaign 2017.

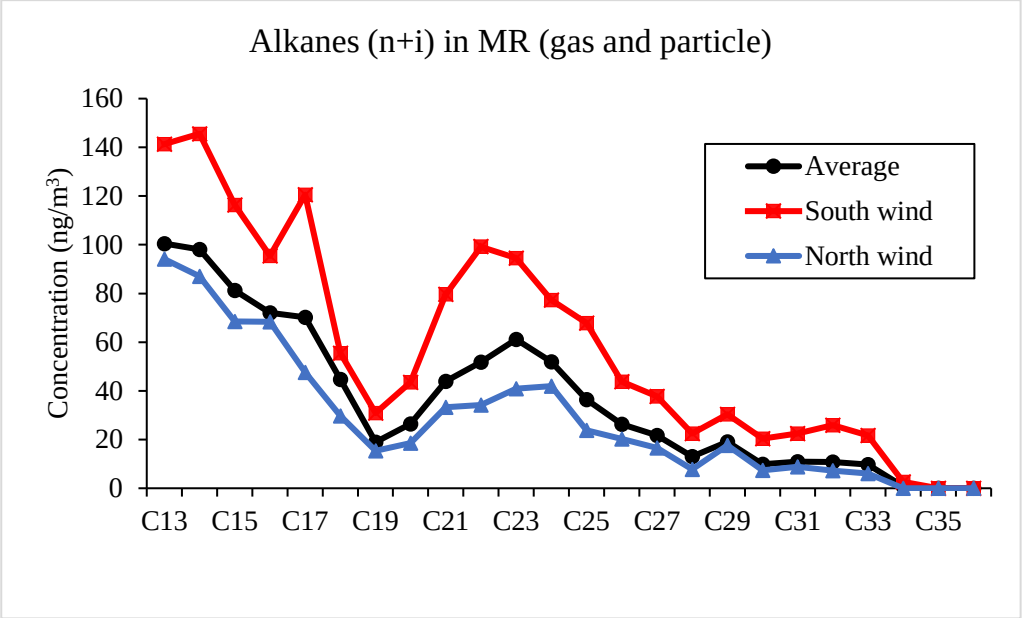

Figure 4: The average alkane (n+i) concentrations in MR (sum of gas phase and particle phase) during the MR campaign during southerly and northerly winds.

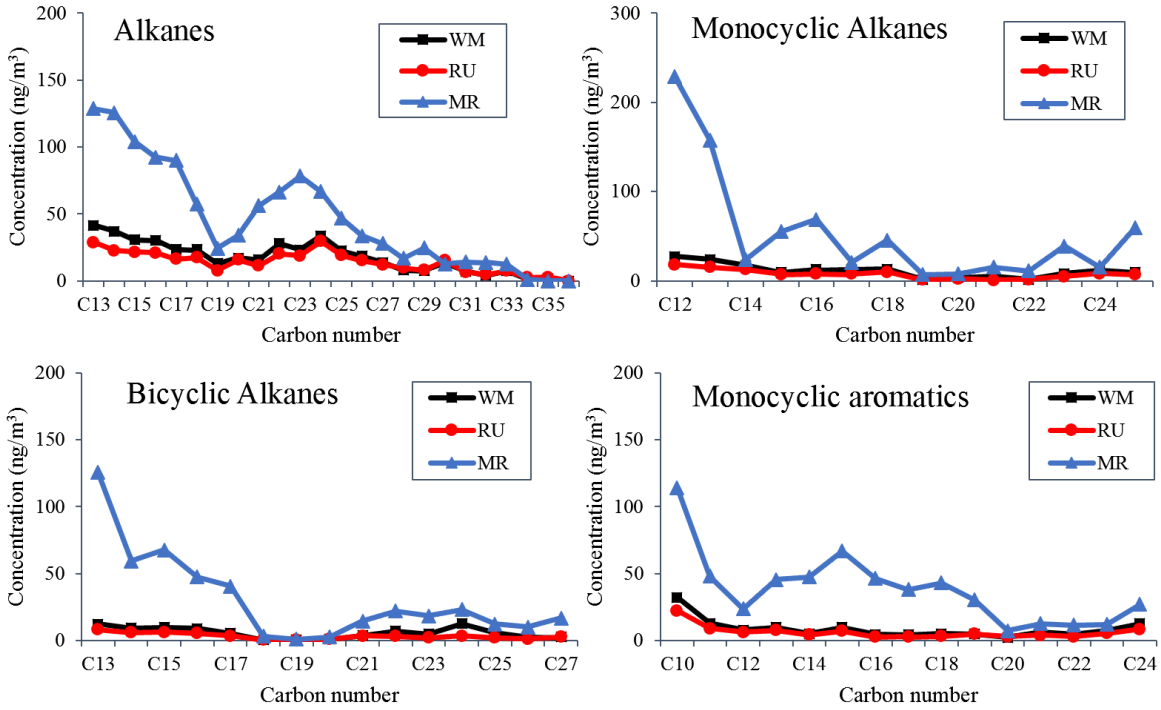

980

981 **Figure 5:** Concentrations of alkanes (n+i), monocyclic alkanes, bicyclic alkanes and monocyclic
982 aromatics (sum of the gas phase and particle phase) at WM and RU measured simultaneously from
983 January to February 2017, together with MR data adjusted to match the same time period (see text).

984

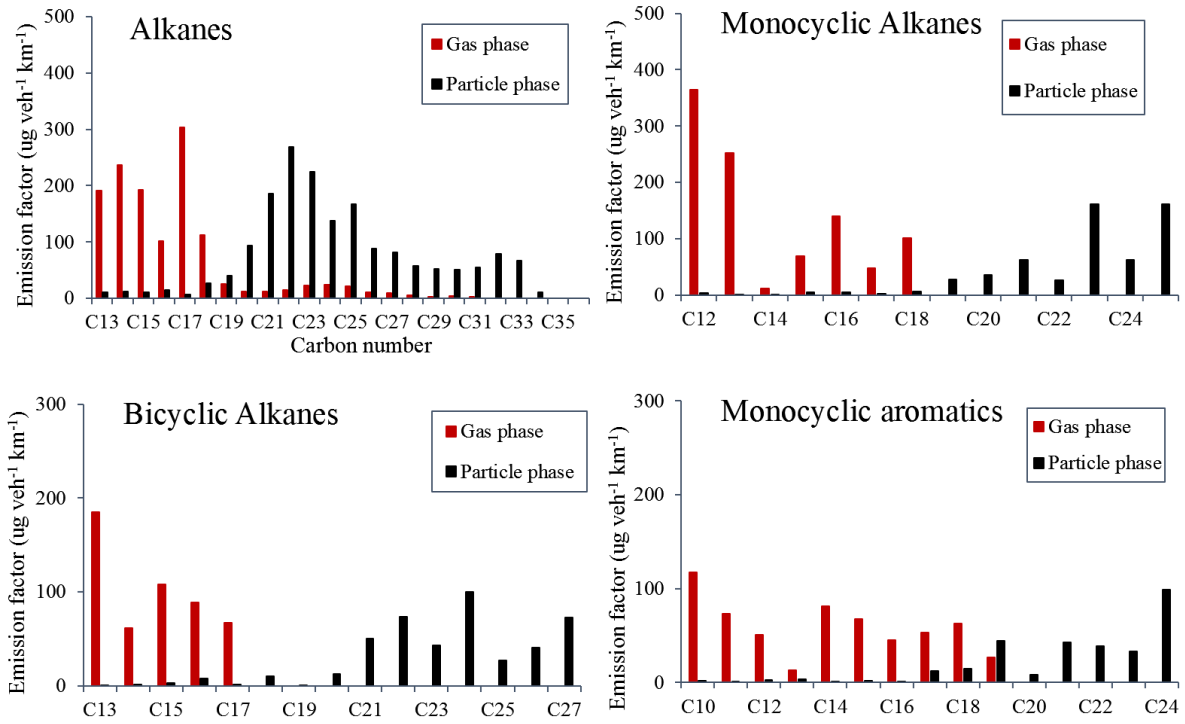

985

986 **Figure 6:** Emission factors of alkanes (n+i), monocyclic alkanes, bicyclic alkanes and monocyclic
987 aromatics in the gas phase and particle phase at MR.

988